

## No phosphine in the atmosphere of Venus

Villanueva G.L., Cordiner, M., Irwin P., de Pater I., Butler B., Gurwell M., Milam S.N., Nixon C. A., Luszcz-Cook S. H., Wilson C., Kofman V., Liuzzi G., Faggi S., Fauchez T., Lippi M., Cosentino R., Thelen A. E., Moullet A., Hartogh P., Molter E.M., Charnley S., Arney G.N., Mandell A.M, Biver N., Vandaele A.C., de Kleer K. R., Kopparapu R.

*Submitted* on October 26<sup>th</sup> 2020 to Nature Astronomy as a “Matters Arising” article

*Submitted* on October 21<sup>st</sup> 2020 to Jane Greaves and Luca Malinaglia (Nature Astronomy editor)

The detection of phosphine (PH<sub>3</sub>) in the atmosphere of Venus has been recently reported employing mm-wave radio observations<sup>1</sup>, hereafter G2020. In this report, we identify several fundamental issues in the analysis and interpretation of the spectroscopic data, which renders this detection of PH<sub>3</sub> invalid. Our recommendation is for the original authors to review the arguments and methods presented here, and once acknowledged, to retract their original claim.

The measurements target the fundamental first rotational transition of PH<sub>3</sub> (J=1-0) at 266.944513 GHz, which was observed with the James Maxwell Clark Telescope (JCMT) in June 2017 and with the Atacama Large Millimeter/submillimeter Array (ALMA) in March 2019. This line is very close to the SO<sub>2</sub> (J=30<sub>9,21</sub>-31<sub>8,24</sub>) transition at 266.943329 GHz (only 1.3 km/s away from the PH<sub>3</sub> line) and therefore this SO<sub>2</sub> line represents a serious source of contamination. The presented JCMT and ALMA datasets as presented in G2020 are at spectral resolutions comparable to the velocity separation of the two lines, and the line cores are several km/s in width, which does not permit spectroscopic separation of these two species.

To explore the hypothesis that the observed 267 GHz feature is SO<sub>2</sub>, and not PH<sub>3</sub>, we employed the same VIR45 temperature/pressure (T/P) profile used by G2020 (“extended Data Figure 8”) and the G2020 SO<sub>2</sub> profile (“extended Data Figure 9”). See further information about plausible Venus SO<sub>2</sub> abundances and known variability in S1. As shown in Figure 1, we can fully explain the claimed “PH<sub>3</sub>” feature with their SO<sub>2</sub> profile. For these simulations, we employed three independent radiative transfer analyses: the Planetary Spectrum Generator (PSG, <https://psg.gsfc.nasa.gov>)<sup>2</sup>, the Non-linear optimal Estimator for Multivariate spectral analysis (NEMESIS)<sup>3</sup> and the CFA planetary modeling tool<sup>4</sup>. The PSG radiative transfer analysis included the latest HITRAN SO<sub>2</sub> line parameters for a CO<sub>2</sub> atmosphere<sup>5</sup>, a layer-by-layer line-by-line study, and a full disk sampling scheme with 10 concentric rings. The NEMESIS analysis was also performed in line-by-line mode, and used the same line data with a 5-point Gauss-Lobatto disc-integration scheme. As described in G2020, there is some uncertainty in the line-shape parameters for the PH<sub>3</sub> line in a CO<sub>2</sub> atmosphere. HITRAN reports an air linewidth of 0.067 cm<sup>-1</sup>/atm for this line, which could correspond to 0.12 cm<sup>-1</sup>/atm for CO<sub>2</sub> if we scale by the typical 1.8 scaling ratio observed for the SO<sub>2</sub> lines<sup>6</sup>. G2020 employed the line shape for the NH<sub>3</sub>(J=1-0) line at 572.498160 GHz, which has a much greater linewidth of 0.2862 cm<sup>-1</sup>/atm. This uncertainty in the linewidth has a dramatic impact on the inferred PH<sub>3</sub> abundance, and our upper limit for the abundance of PH<sub>3</sub> from these data (after removing SO<sub>2</sub>) ranges from < 5 ppb (3σ) for 0.12 cm<sup>-1</sup>/atm to < 12 ppb (3σ) for 0.2862 cm<sup>-1</sup>/atm (Figure 1). This upper-limit is consistent with the recent reports of non-detection of PH<sub>3</sub> (< 5 ppb) at infrared wavelengths with TEXES/NASA-IRTF<sup>7</sup>.

The analysis of interferometric data is relatively complex, in particular for such a bright and extended source as Venus (15.4 arcsecs angular diameter for the data ALMA data in G2020). The completeness of the different baselines (short and long) defines the accuracy in capturing the disk fluxes<sup>8</sup>, while the bandpass calibration is a crucial factor in the ultimate quality of the resulting spectra<sup>9,10</sup>. How these parameters are treated and defined in the calibration scripts can have a dramatic impact on the quality and validity of the resulting ALMA interferometric data. The extracted spectra in “extended Figure 4” and interferometric map in “extended Figure 3” of G2020 show strong fringing patterns within the PH<sub>3</sub> region. Particularly problematic is the fact that this fringing has a pattern/width comparable to their defined  $\pm 5$  km/s PH<sub>3</sub> line core region; as we present in S2, artificial features can easily be produced when removing high-order polynomials from these residual data<sup>11</sup>.

Many of these extraneous features are introduced by the selection of baselines and the parameters considered in the calibration scripts. For instance, we noticed notable differences in the residual spectra and the fringing quality/pattern when we enable the “usescratch=True” setting in CASA’s `setJy` when compared to the G2020 calibration script without this feature. This issue has been officially flagged by the ALMA NASSC, and the JAO has taken a decision to re-evaluate these data in QA3. Independent processing of the ALMA data by several teams (e.g., NASA/GSFC, Berkeley, NRAO) leads to residual spectra with less notable fringing. We analyzed the data employing two separate analysis packages: the ALMA/CASA pipeline (with corrected scripts), and the Astronomical Image Processing System (AIPS). For the analysis, we took the data from the ALMA calibration pipeline, recalibrated the bandpass, self-calibrated Venus, subtracted the continuum, made an image cube, and formed a disk-averaged spectrum, shown in Figure 2. When employing AIPS, we found no need to exclude short baselines, and no need to fit a high-order “continuum baseline” in the disk-averaged spectrum – the resulting spectrum is flat, to the noise level (see Figure FS3). Ultimately, our analysis of the data using several different approaches reveals no signature of PH<sub>3</sub>, leading to an upper-limit of  $< 1$  ppb ( $3\sigma$ ) for  $0.12 \text{ cm}^{-1}$  to  $< 2$  ppb ( $3\sigma$ ) for  $0.2862 \text{ cm}^{-1}/\text{atm}$  (Figure 2). We further validate our analysis of the ALMA data by probing the abundances of SO<sub>2</sub> and HDO employing nearby lines, see S3.

Additionally, there is a fundamental mismatch between the inferred vertical profile of PH<sub>3</sub> from the data done by G2020 with their predictions of the photochemical model employed to interpret them. The narrow features of PH<sub>3</sub> and SO<sub>2</sub> at these frequencies sample the middle/upper atmosphere of Venus. Considering a typical linewidth of  $\sim 0.2 \text{ cm}^{-1}/\text{atm}$  for a CO<sub>2</sub> atmosphere, this would correspond to  $\sim 6$  GHz of linewidth at 1 bar, and the narrow linewidths of  $\pm 5$  km/s claimed in G2020 can only be ascribed to altitudes above 70 km ( $< 2 \times 10^{-2}$  bar,  $< 110$  km/s width). Therefore, any molecular abundance below this altitude range would only contribute to the continuum, which is removed by their polynomial fitting scheme. This indicates a major inconsistency between the photochemical model results for PH<sub>3</sub> presented in “extended Data Figure 9” ( $< 65$  km) and the data ( $> 70$  km). The photochemical results in G2020 indicate  $< 0.001$  ppb of PH<sub>3</sub> at  $> 70$  km, much lower than the 20 ppbv suggested to be present for the assumed deeper altitudes. Thus, the photochemical modeling predictions do not match the PH<sub>3</sub> abundances at the correct altitudes, and significantly higher production rates would be required to produce PH<sub>3</sub> at the claimed abundances of G2020 for  $> 70$  km, calling into question the claimed photochemical network for these results.

In summary, we demonstrate that the observed JCMT feature can be fully modeled employing plausible mesospheric SO<sub>2</sub> abundances (~100 ppbv as per the SO<sub>2</sub> profile given in G2020's extended figure 9), while the identification of PH<sub>3</sub> in the ALMA data should be considered invalid due to severe baseline calibration issues. Furthermore, for any PH<sub>3</sub> signature to be produced in either ALMA or JCMT spectra, PH<sub>3</sub> needs to present at altitudes above 70 km, in stark disagreement with the G2020 photochemical network. We ultimately conclude that this detection of PH<sub>3</sub> in the atmosphere of Venus is incorrect and invite the Greaves et al. team to revise their work and consider a correction or retraction of their original report.

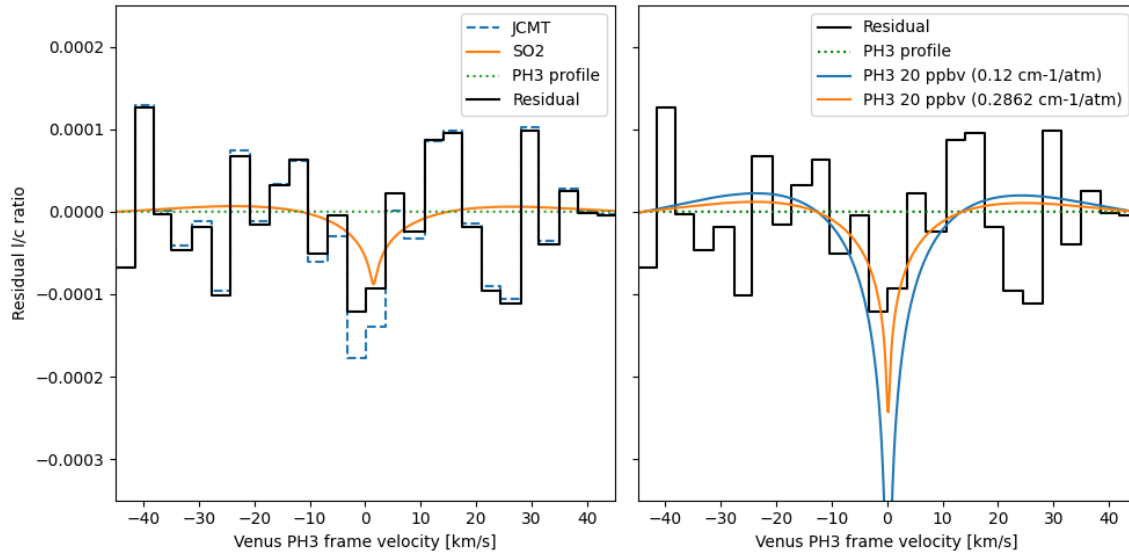


**Figure 1:** Comparison between the residual JCMT data as presented in Figure 1 of G2020 and models of  $\text{SO}_2$  and  $\text{PH}_3$ . **Left:** The JCMT data (Figure 1 of G2020) for their most conservative polynomial solution is shown with a dashed blue trace. “ $\text{SO}_2$ ” is a model spectrum synthesized using their T/P (G2020, Figure 8) and their  $\text{SO}_2$  profile (G2020, Figure 9,  $\sim 100$  ppbv in the 70-90 km region), while  $\text{PH}_3$  is a model spectrum using their  $\text{PH}_3$  profile (G2020, Figure 9). The residual of the data minus the  $\text{SO}_2$  model is shown as a black trace, leading to no significant remnant signal. **Right:** Comparison of the residual JCMT spectrum (after removing  $\text{SO}_2$ ) to three models of  $\text{PH}_3$ . The green dotted line shows a model assuming their  $\text{PH}_3$  profile, while the orange and blue lines assume a constant 20 ppbv abundance ratio across all altitudes, where the orange line model uses their assumed linewidth ( $0.2862 \text{ cm}^{-1}/\text{atm}$ ) and blue model assumes the HITRAN air-broadened value scaled by 1.8 ( $0.12 \text{ cm}^{-1}/\text{atm}$ ).

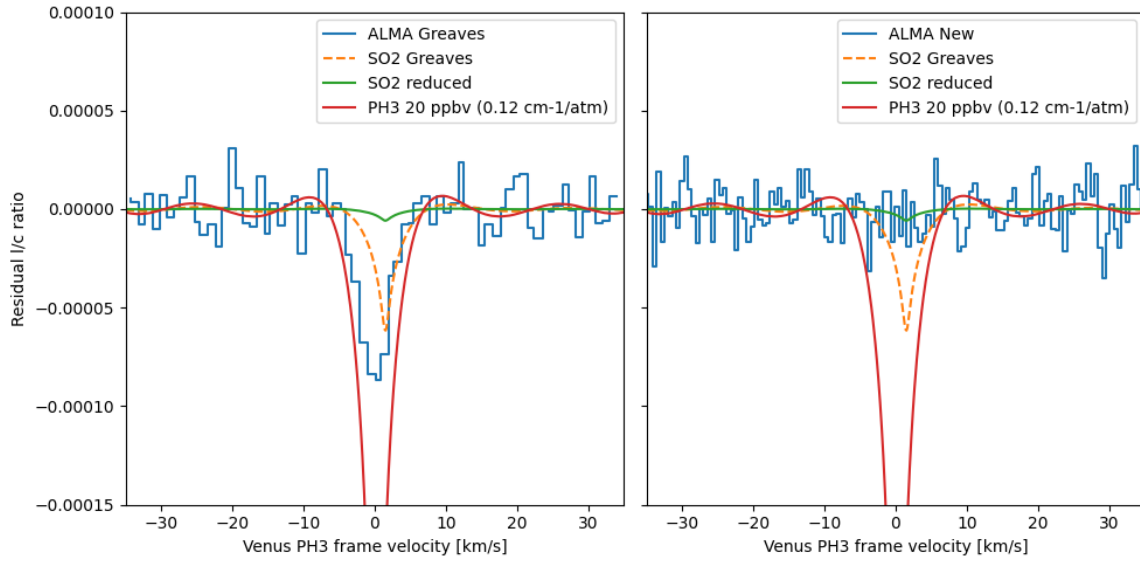


**Figure 2:** Comparison between ALMA data (G2020 and our independently processed) with models of  $\text{SO}_2$  and  $\text{PH}_3$ . **Left:** The ALMA data as presented in Figure 2 of G2020 for the whole planet, while “ $\text{SO}_2$  Greaves” is a synthetic spectrum as modeled using their T/P (G2020 Figure 8) and their  $\text{SO}_2$  profile (G2020 Figure 9,  $\sim 100$  ppbv in the 70-90 km region). “ $\text{SO}_2$  reduced” is a model with a reduced mesospheric  $\text{SO}_2$  ( $\sim 10$  ppbv in the 70-90 km region) matching the nearby ( $J=13_{3,11}-13_{2,12}$ ) line at 267.537458 GHz (see Figure 4) – abundances comparable to those reported by Encrenaz et al. (2015). The  $\text{PH}_3$  model shown employs a constant 20 ppbv abundance ratio across all altitudes, with a linewidth of  $0.12 \text{ cm}^{-1}/\text{atm}$ . **Right:** Same as the left panel but showing the newly processed data employing the default ALMA pipeline.

## **Supplementary material**

### **S1: Vertical profiles**

The temperature profile as presented in “extended Data Figure 8” of G2020 is consistent with the Venus International Reference Atmosphere (VIRA)<sup>13</sup> for mid-latitudes (45 degrees latitude), and also consistent with later observations<sup>14</sup>. Their SO<sub>2</sub> profile, in particular at altitudes above 70 km relevant to this investigation, in “extended Data Figure 9” is consistent with previous observations<sup>15–17</sup>. Yet, SO<sub>2</sub> is known to vary greatly temporally and spatially<sup>12,16–18</sup>, ranging from <10 to >200 ppbv in the 70–100 km altitude region. Large variations have been observed on timescales of hours to months<sup>12</sup>, so mesospheric SO<sub>2</sub> abundances at the time of the JCMT observations in June 2017 cannot be constrained by SO<sub>2</sub> abundances measured using ALMA in March 2019. The reported SO<sub>2</sub> profile in “extended Data Figure 9” of ~100 ppbv in the 70–90 km altitude range can then be assumed to be a plausible and average value for SO<sub>2</sub>.

### **S2: Analysis of the ALMA using G2020 calibration scripts**

We investigated their data present on the archive, and analyzed it using the original pipeline calibration (G2020 Supplementary Software 2, 3). We mapped Venus including all baselines, subtracted the continuum emission using the `uvcontsub` task in CASA, and produced the spectrum in Figure FS1(left) integrated over Venus, including its limb. We then overlaid two 12<sup>th</sup> order polynomial fits: the blue one a fit to the entire spectrum, and the red one excluding the center 10 km/s (i.e., from -5 to +5 km/s), as done in G2020. The right panel shows the spectra after subtracting the polynomial fits (blue for the blue polynomial, red for the red one). As expected, a feature shows up in the red spectrum, i.e., part of the original dip in the bandpass. This process clearly shows that with harmonics in the bandpass as observed, subtracting polynomial fits to part of the data may create line profiles that might be confused with real lines.

### **S3: Validation of our ALMA analysis by interpreting other nearby lines**

We independently analyzed the ALMA data using our calibration scripts for the region near the SO<sub>2</sub> line at 267.537458 GHz and the HDO (J=2<sub>2,0</sub>-3<sub>1,3</sub>) line at 266.16107 GHz (Figure FS2). From these data, we obtain a mesospheric SO<sub>2</sub> abundance value of ~10 ppb, lower than that specified in the G2020 “extended Data Figure 9” yet well within the range previously reported SO<sub>2</sub> abundances from ALMA observations at 346.652167 GHz<sup>12</sup> and comparable to the value retrieved from this line by G2020. This level of variability observed between JCMT, ALMA, and previous ALMA measurements is also consistent with previous reports of the SO<sub>2</sub> temporal/spatial variability<sup>12,16–18</sup>. Similarly for HDO, we also observe a consistent set of data and model results when employing a plausible water profile and assuming a D/H of 200<sup>19</sup>.

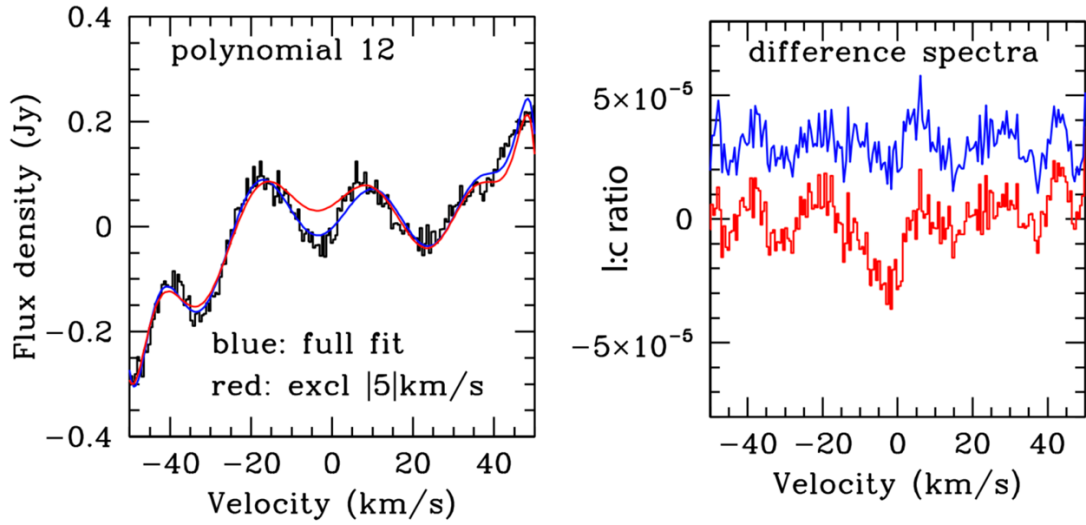


**Figure FS1:** **Left:** Disk-integrated spectrum of Venus (including its limb) as constructed from the data used in G2020 (but without deleting short spacings). Polynomial fits (12<sup>th</sup> order) are superposed: “blue” trace is a fit to the entire spectrum, while “red” is a fit excluding the center -5 to +5 km/s. **Right:** Spectra after subtracting the polynomial fits (red: subtracting red polynomial; blue: subtracting blue polynomial).

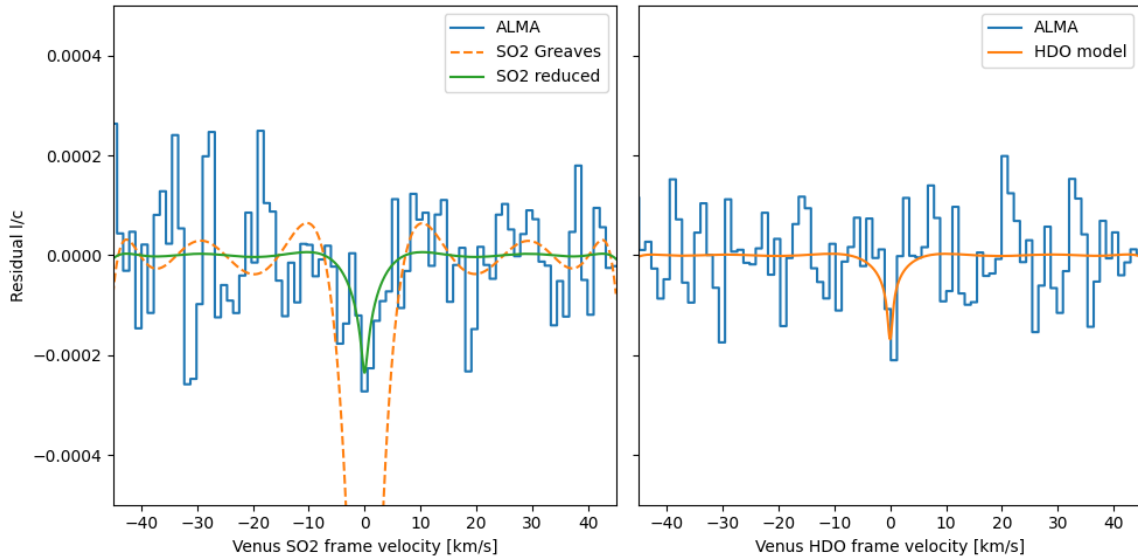


**Figure FS2:** Comparison between models and ALMA data, as presented in Figure 4 of G2020, for the SO<sub>2</sub> ( $J=13_{3,11}-13_{2,12}$ ) transition at 267.537458 GHz and for the HDO ( $J=2_{2,0}-3_{1,3}$ ) transition at 266.161070 GHz. **Left:** Our independently processed ALMA data for the SO<sub>2</sub> line, while “SO<sub>2</sub> Greaves” is a synthetic spectrum modeled using their T/P (G2020 Figure 8) and their SO<sub>2</sub> profile (G2020 Figure 9), “SO<sub>2</sub> reduced” is a model with reduced mesospheric SO<sub>2</sub> levels ( $\sim 10$  ppb in the 70-90 km range) and comparable to those reported by <sup>12</sup>. **Right:** Our independently processed ALMA data for a nearby HDO line presented, while “HDO model” is a synthetic spectrum as modeled using their T/P (their figure 8), a D/H of 200<sup>19</sup>, and plausible H<sub>2</sub>O abundances of  $\sim 60$  ppbv in the mesosphere (70-100 km).

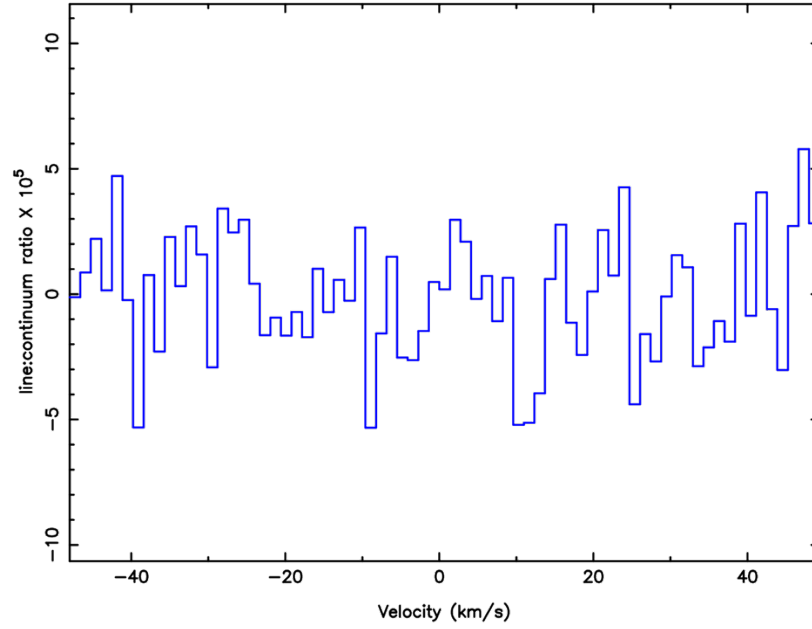


**Figure FS3:** Disk-averaged spectrum in the PH<sub>3</sub> narrow spectral window, after re-reduction in AIPS. No PH<sub>3</sub> line is detected.



## References

1. Greaves, J. S. *et al.* Phosphine gas in the cloud decks of Venus. *Nat. Astron.* 1–10 (2020) doi:10.1038/s41550-020-1174-4.
2. Villanueva, G. L., Smith, M. D., Protopapa, S., Faggi, S. & Mandell, A. M. Planetary Spectrum Generator: An accurate online radiative transfer suite for atmospheres, comets, small bodies and exoplanets. *J. Quant. Spectrosc. Radiat. Transf.* **217**, 86–104 (2018).
3. Irwin, P. G. J. *et al.* The NEMESIS planetary atmosphere radiative transfer and retrieval tool. *J. Quant. Spectrosc. Radiat. Transf.* **109**, 1136–1150 (2008).
4. Gurwell, M. A., Bergin, E. A., Melnick, G. J. & Tolls, V. Mars surface and atmospheric temperature during the 2001 global dust storm. *Icarus* **175**, 23–31 (2005).
5. Gordon, I. E. *et al.* The HITRAN2016 molecular spectroscopic database. *J. Quant. Spectrosc. Radiat. Transf.* **203**, 3–69 (2017).
6. Wilzewski, J. S., Gordon, I. E., Kochanov, R. V., Hill, C. & Rothman, L. S. H<sub>2</sub>, He, and CO<sub>2</sub> line-broadening coefficients, pressure shifts and temperature-dependence exponents for the HITRAN database. Part 1: SO<sub>2</sub>, NH<sub>3</sub>, HF, HCl, OCS and C<sub>2</sub>H<sub>2</sub>. *J. Quant. Spectrosc. Radiat. Transf.* **168**, 193–206 (2016).
7. Encrenaz, T. *et al.* A stringent upper limit of the PH<sub>3</sub> abundance at the cloud top of Venus. *ArXiv201007817 Astro-Ph* (2020).
8. Pater, I. de *et al.* First ALMA Millimeter-wavelength Maps of Jupiter, with a Multiwavelength Study of Convection. *Astron. J.* **158**, 139 (2019).
9. Thelen, A. E. *et al.* Detection of CH<sub>3</sub>CS<sub>3</sub>N in Titan's Atmosphere. (2020).
10. Yamaki, H., Kamenno, S., Beppu, H., Mizuno, I. & Imai, H. Optimization by Smoothed Bandpass Calibration in Radio Spectroscopy. *Publ. Astron. Soc. Jpn.* **64**, (2012).
11. Snellen, I. A. G., Guzman-Ramirez, L., Hogerheijde, M. R., Hygate, A. P. S. & van der Tak, F. F. S. Re-analysis of the 267-GHz ALMA observations of Venus: No statistically significant detection of phosphine. *ArXiv201009761 Astro-Ph* (2020).
12. Encrenaz, T., Moreno, R., Moullet, A., Lellouch, E. & Fouchet, T. Submillimeter mapping of mesospheric minor species on Venus with ALMA. *Planet. Space Sci.* **113–114**, 275–291 (2015).
13. Seiff, A. *et al.* Models of the structure of the atmosphere of Venus from the surface to 100 kilometers altitude. *Adv. Space Res.* **5**, 3–58 (1985).
14. Limaye, S. S. *et al.* Venus Atmospheric Thermal Structure and Radiative Balance. *Space Sci. Rev.* **214**, 102 (2018).
15. Vandaele, A. C. Composition and Chemistry of the Neutral Atmosphere of Venus. *Oxford Research Encyclopedia of Planetary Science* <https://oxfordre.com/planetaryscience/view/10.1093/acrefore/9780190647926.001.0001/acrefore-9780190647926-e-4> (2020) doi:10.1093/acrefore/9780190647926.013.4.
16. Vandaele, A. C. *et al.* Sulfur dioxide in the Venus atmosphere: I. Vertical distribution and variability. *Icarus* **295**, 16–33 (2017).
17. Vandaele, A. C. *et al.* Sulfur dioxide in the Venus Atmosphere: II. Spatial and temporal variability. *Icarus* **295**, 1–15 (2017).
18. Marcq, E. *et al.* Climatology of SO<sub>2</sub> and UV absorber at Venus' cloud top from SPICAV-UV nadir dataset. *Icarus* **335**, 113368 (2020).
19. Piccialli, A. *et al.* Mapping the thermal structure and minor species of Venus mesosphere with ALMA submillimeter observations. *Astron. Astrophys.* **606**, A53 (2017).